

JGR Biogeosciences

RESEARCH ARTICLE

10.1029/2018JG004961

Key Points:

- Vadose zone CO₂ dynamics are strongly influenced by changes in atmospheric pressure
- Vadose zone CO₂ shows fluctuations of up to 2000 ppm in less than 6 hours. The dominant periods range from 0.5 to ~30 days
- The underlying physical mechanism is related to pressure tides

Correspondence to:

M. R. Moya,
charo.moya@eeza.csic.es

Citation:

Moya, M. R., Sánchez-Cañete, E. P., Vargas, R., López-Ballesteros, A., Oyonarte, C., Kowalski, A. S., et al. (2019). CO₂ dynamics are strongly influenced by low frequency atmospheric pressure changes in semiarid grasslands. *Journal of Geophysical Research: Biogeosciences*, 124, 902–917. <https://doi.org/10.1029/2018JG004961>

Received 28 NOV 2018

Accepted 28 JAN 2019

Accepted article online 4 FEB 2019

Published online 12 APR 2019

Author Contributions:

Conceptualization: E. P. Sánchez-Cañete, C. Oyonarte, A. S. Kowalski, P. Serrano-Ortiz, F. Domingo

Data curation: M. R. Moya, E. P. Sánchez-Cañete, A. López-Ballesteros, P. Serrano-Ortiz

Formal analysis: M. R. Moya, E. P. Sánchez-Cañete, R. Vargas, A. López-Ballesteros

Funding acquisition: E. P. Sánchez-Cañete, R. Vargas, A. S. Kowalski, P. Serrano-Ortiz, F. Domingo

Investigation: M. R. Moya

Methodology: E. P. Sánchez-Cañete, A. S. Kowalski









Resources: E. P. Sánchez-Cañete, C. Oyonarte, A. S. Kowalski, P. Serrano-Ortiz, F. Domingo

Supervision: E. P. Sánchez-Cañete, R. Vargas, F. Domingo

Writing - original draft: M. R. Moya

Writing - review & editing: M. R. Moya, E. P. Sánchez-Cañete, R. Vargas, (continued)

CO₂ Dynamics Are Strongly Influenced by Low Frequency Atmospheric Pressure Changes in Semiarid Grasslands

M. R. Moya¹ , E. P. Sánchez-Cañete^{2,3} , R. Vargas⁴ , A. López-Ballesteros⁵ ,
C. Oyonarte^{6,7} , A. S. Kowalski^{2,3} , P. Serrano-Ortiz^{3,8} , and F. Domingo¹ 

¹Department of Desertification and Geo-ecology, Experimental Station of Arid Zones (EEZA-CSIC), Almeria, Spain,

²Department of Applied Physics, University of Granada, Granada, Spain, ³Andalusian Institute for Earth System Research (IIETA), Granada, Spain, ⁴Department of Plant and Soil Sciences, University of Delaware, Newark, Delaware, USA,

⁵Department of Botany, Trinity College Dublin, School of Natural Sciences, Dublin, Ireland, ⁶Department of Agronomy, University of Almeria, Almeria, Spain, ⁷Andalusian Centre for the Assessment and Monitoring of Global Change (CAESCG), Almeria, Spain, ⁸Department of Ecology, University of Granada, Granada, Spain

Abstract Due to their large carbon storage capacity and ability to exchange subterranean CO₂ with the atmosphere, soils are key components in the carbon balance in semi-arid ecosystems. Most studies have focused on shallow (e.g., <30 cm depth) soil CO₂ dynamics neglecting processes in deeper soil layers where highly CO₂-enriched air can be stored or transported through soil pores and fissures. Here, we examine the relationship among variations in subterranean CO₂ molar fraction, volumetric water content, soil temperature and atmospheric pressure during three years within soil profiles (0.15, 0.50, and 1.50 m depths) in two semi-arid grasslands located in southeastern Spain. We applied a wavelet coherence analysis to study the temporal variability and temporal correlation between the CO₂ molar fraction and its covariates (soil temperature, soil moisture and atmospheric pressure). Our results show that CO₂ dynamics are strongly influenced by changes in atmospheric pressure from semidiurnal, diurnal and synoptic to monthly time-scales for all soil depths. In contrast, only weak daily dependencies were found at the surface level (0.15 m) regarding soil temperature and volumetric water content. Atmospheric pressure changes substantially influence variations in the CO₂ content (with daily fluctuations of up to 2000 ppm) denoting transportation through soil layers. These results provide insights into the importance of subterranean storage and non-diffusive gas transport that could influence soil CO₂ efflux rates, processes that are not considered when applying the flux-gradient approach and, which can be especially important in ecosystems with high air permeability between the unsaturated porous media and the atmosphere.

Plain Language Summary Each type of ecosystem has a role in the balance of atmospheric greenhouse gases, acting as either sink or source. Semi-arid ecosystems occupy approximately 40% of the terrestrial surface and dominate the trend and variability of the land CO₂ sink. The roles played by such ecosystems remain under-investigated, and the resulting lack of knowledge undermines future predictions of global environmental change. This study shows that underground CO₂ dynamics in two semi-arid ecosystems are strongly influenced by changes in atmospheric pressure (with strong daily fluctuations), while only weak dependencies were found regarding soil temperature and water content (factors that affect biologic activity). The atmospheric pressure effect on the soil CO₂ concentration was more evident when the air permeability between atmosphere and soil surface was higher. Soil CO₂ variations forced by changes in atmospheric pressure occur consistently from semidiurnal to monthly time-scales. These observations will help to improve the current models that assume soil temperature and moisture to be the main drivers of soil CO₂ dynamics, but are mistakenly applied in semi-arid ecosystems.

1. Introduction

Semi-arid ecosystems occupy approximately 40% of the terrestrial surface and are home to more than 38% of the total global population (Reynolds et al., 2007), but they are under-represented in ecological research networks (Reichstein et al., 2013; Schimel, 2010; Villarreal et al., 2018). In these ecosystems, soils play a key role in the uptake and emissions of the main greenhouse gases (Ahlström et al., 2015; Poulter et al., 2014). Unfortunately, most studies have focused on shallow soil CO₂ dynamics (<30 cm depth) neglecting what occurs in deeper soil layers. The vadose zone may contain large amounts of CO₂-enriched air in pores,

A. López-Ballesteros, C. Oyonarte, A. S. Kowalski, P. Serrano-Ortiz, F. Domingo

cracks and fissures with concentrations higher than 5% by volume in the first tens of meters (Benavente et al., 2010; Denis et al., 2005). Soil CO₂ content is characterized by a vertical profile of concentration increasing with depth, that is affected by the transport of dissolved atmospheric and soil CO₂ in waters and gravitational percolation (Baldini et al., 2006; Sánchez Cañete, Ortiz, et al., 2013) where deeper soil layers can reach *c.a.* 100 times more CO₂ content than shallower layers (Buyanovsky & Wagner, 1983). This CO₂-enriched air stored in the soil pores shows clear seasonal and daily patterns of variation driven by a set of biological, physical and chemical processes that are involved in CO₂ production and transport that ultimately influence soil CO₂ efflux rates to the atmosphere.

The diffusion process, driven by a gradient of molar fraction, is considered the main mechanism of gas exchange between the atmosphere and vadose zone (including shallow horizon and deep soil layers; Rolston & Moldrup, 2012). Advective gas transport, driven by bulk flow acting on a concentration gradient, can also strongly affect soil gas migration (Corey et al., 2010; Garcia-Anton et al., 2014). Both transport processes are highly interconnected. Diffusion is a slow transport process modeled by Fick's first law (only dependent on soil CO₂ production and diffusivity; Maier & Schack-Kirchner, 2014), while bulk flow is typically modeled using Darcy's law (Webb, 2006). Non-diffusive transport processes are usually not considered in the flux model calculations (Maier et al., 2010; Webb & Pruess, 2003). Although its effect is limited in time (Maier et al., 2010), non-diffusive transport can also participate, increasing the gas exchange rates, which results in a more efficient transport mechanism compared to molecular diffusion alone (Bowling & Massman, 2011; Maier et al., 2012; Roland et al., 2015; Takle et al., 2004).

Non-diffusive and diffusive transport processes can be affected by several abiotic factors, such as volumetric water content (Martinez & Nilson, 1999), soil temperature (Roland et al., 2015), gas content (Elberling et al., 1998), soil texture (Kimball & Lemon, 1971), soil porosity (Nilson et al., 1991; Takle et al., 2004), wind (Bowling & Massman, 2011; Kowalski et al., 2008; Sanchez-Cañete et al., 2011), water table fluctuations (Jiao & Li, 2004; Maier et al., 2010) or atmospheric pressure. The movement of CO₂-enriched air driven by pressure changes is also known as pressure pumping. The potential relevance of non-diffusive transport caused by pressure pumping has been mostly addressed at short time-scales (< 1 s; Kimball & Lemon, 1970; Massman et al., 1997; Mohr et al., 2016; Takle et al., 2004), although it also has been studied at half-hourly and longer temporal scales (Bowling & Massman, 2011; Clements & Wilkening, 1974; Elberling et al., 1998; Sánchez Cañete, Kowalski, et al., 2013). To a lesser extent, pressure oscillations produced at low frequency scales have also been termed as atmospheric or pressure tides (Kuang et al., 2013; Le Blancq, 2011; Lindzen, 1979; Massmann & Farrier, 1992). Through this pressure fluctuation, the direction and magnitude of soil gas efflux can be altered substantially (Bowling & Massman, 2011; Takle et al., 2004). This phenomenon can be more relevant in carbonated ecosystems, where the presence of fissures and cavities increases the degree of permeability between deeper layers and the soil surface (Cuezva et al., 2011; Serrano Ortiz et al., 2010), increasing pressure pumping and pressure tides effects.

This study focuses on how CO₂ dynamics in the vadose zone is affected by changes in environmental and subterranean conditions by comparing two nearby semi-arid grassland sites. For that, we used a 3-year (2014–2016) record of edaphic (soil profile at 0.15 m, 0.50 m and 1.50 m) and environmental variables. We hypothesize that due to the scarce vegetation and impoverished soils (Lithic Leptosols with thin soil depth and low content in soil organic carbon; IUSS Working Group WRB, 2015), and the dry conditions of the layers (generally volumetric water content <10%), variations in the vadose zone CO₂ molar fraction will be dominated by abiotic factors. We expect that atmospheric pressure will be the main environmental variable influencing CO₂ dynamics at daily and weekly time-scales because pressure differences in permeable soils could enhance CO₂ transport. A better understanding about the driving factors determining CO₂ dynamics, as well as their temporality, is especially relevant to improve future models related with subterranean CO₂ storage and non-diffusive gas transport in the vadose zone.

2. Material and Methods

2.1. Study Site

The study area is located in Cabo de Gata-Níjar Natural Park, in the province of Almeria in the SE of Spain. We selected two neighboring semi-arid grassland sites similar in terms of climate, geology, topography and

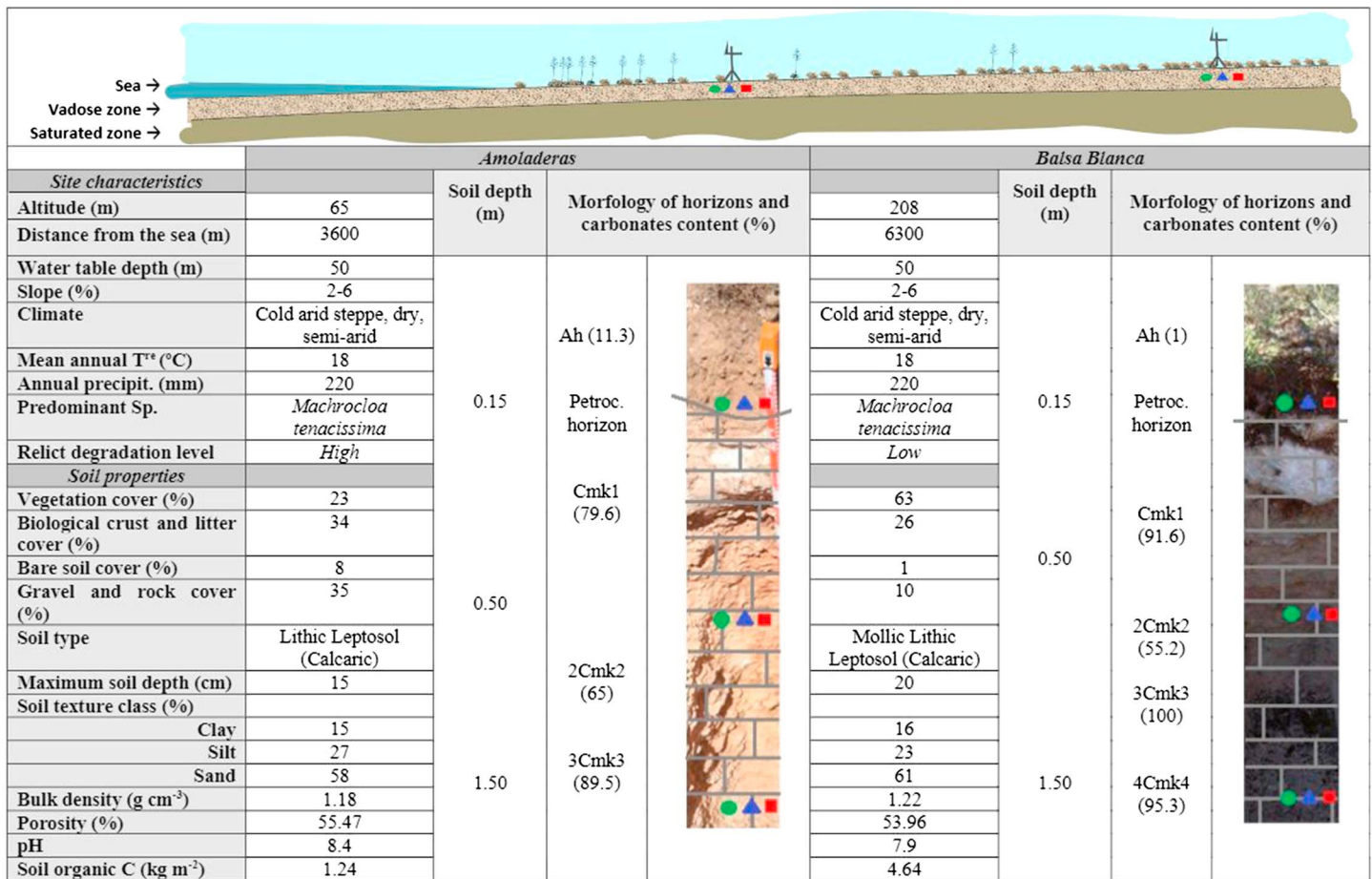


Figure 1. Description of site and soils characteristics in Amoladeras and Balsa Blanca. The information is coupled with a schematic illustration of our experimental design. Soil molar fraction sensors, soil thermistors and volumetric water content reflectometers are represented as geometric figures. Pedological characteristics (pedogenic maximum depth and petrocalcic horizon) are represented with drawn lines. Morphological horizons are described according to (FAO, 2009). Water table depth is determined from (Junta de Andalucía, C. d. M. A. y. O. d. T, 2013).

vegetation: (1) Balsa Blanca (N36°56'26.8" W2°01'58.8"; hereinafter BB), and (2) Amoladeras (N36°50'5" W2°15'1"; hereinafter AM). However, the footprint of past degradation, likely due to grazing (Alados et al., 2004), is more evident in AM (López-Ballesteros et al., 2018; Rey et al., 2011). The area is classified as a hot arid desert according to Köppen classification (BWh; Rubel & Kottek, 2010). The climate is characterized by a mean annual precipitation of 220 mm and a mean annual temperature of 18 °C (Figure 1). Climatic conditions are also characterized by a long dry season, which begins in June and ends abruptly in September–October with rain pulse events (López Ballesteros et al., 2016). At our experimental sites, geological materials consist of a quaternary conglomerates and Neogene-Quaternary sediments cemented by lime (caliche). The limestone crust is located on a glacia. The glacia in AM has pinkish silts and quartz boulders from the Upper Pleistocene; while in BB it is a calcareous crust “dalle” low detritic from the Lower Pleistocene (MAGNA, 2010). Both sites are located geomorphologically on a flat alluvial fan of gentle slopes (2–6%) with petrocalcic horizons (i.e., caliche). Petrocalcic horizons are characterized by bulk densities ranging between 1.6 and 2.3 g cm⁻³ and porosities ranging between 16 and 40% (Duniway et al., 2007; Zamanian et al., 2016). The characteristics of these materials depend on origin, formation processes and morphology of pedogenic carbonates (Zamanian et al., 2016) producing discontinuities through the vertical layers that are unknown in our experimental sites. In the surface soil horizon, bulk density is lower (1.18–1.22 g cm⁻³) and porosity is much higher (55.47–53.96%). The water table is at 50 m depth approximately (Junta de Andalucía, C. d. M. A. y. O. d. T, 2013). The dominant soils are classified as Lithic Leptosols (IUSS Working Group WRB, 2015); they are shallow (10–20 cm) and alkaline (pH 7.9–8.4), with sandy loam texture class and carbonate saturated (Figure 1). Vegetation is dominated by *Macroclia tenacissima*

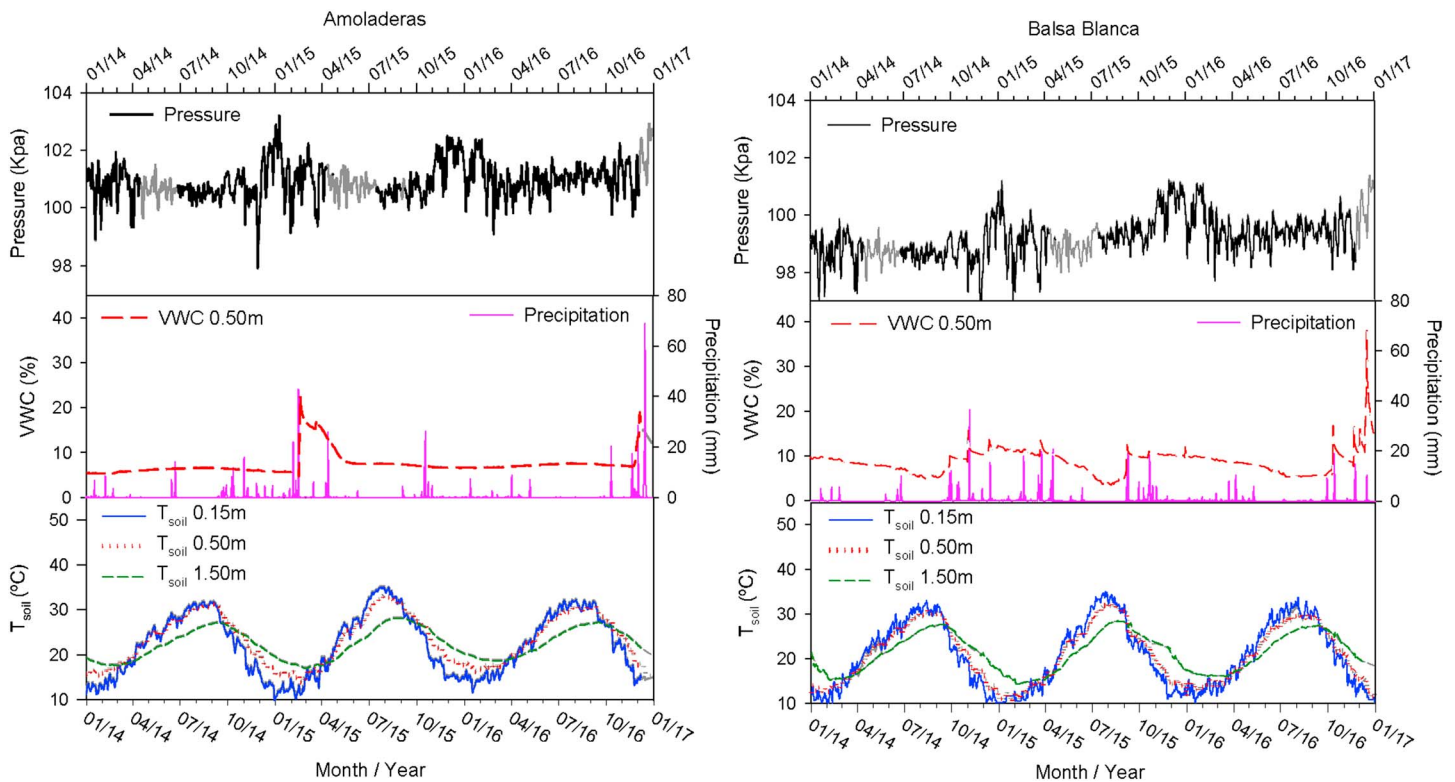


Figure 2. Daily-averaged values of atmospheric pressure, volumetric water content (VWC) at 0.50 m, soil temperature (T_{soil}) at soil depths of 0.15 m (solid lines), 0.50 m (dotted lines) and 1.50 m (dashed lines); and daily precipitation during the study period (January 2014–December 2016). Shaded lines represent gaps in the time series.

(previously known as *Stipa tenacissima*) and other drought-tolerant plant species. In the soil surface there are patches of bare soil, sections with biological soil crusts, and exposed gravel and rock outcrops. Absolute pressure in AM (65 m in altitude) is greater than in BB (208 m in altitude) by about 2 kPa (Figure 2). The sites are 23 km apart, and AM is closer to the coast (Figure 1).

2.2. Experimental Design

Vertical profiles were installed in January 2010 in BB and in July 2013 in AM. Boreholes were done with an excavator and the extracted material was used for refilling. The study period covered from January 2014 to December 2016, rejecting a stabilization period of 6 months after the installation of the vertical profile in AM (July 2013). The stabilization period was selected after comparing CO_2 dynamics in both vertical profiles. Vertical profiles measured soil CO_2 molar fractions (χ_c ; infra-red sensor GMP-343, Vaisala, Inc., Finland), soil temperatures (T_{soil} ; 107 thermistors, Campbell Scientific, Logan, UT, USA) and volumetric soil water content (VWC; TDR, CS616, Campbell Scientific, Logan, UT, USA). Sensors were installed horizontally in undisturbed media at three different depths: 0.15 m soil horizons (belonging to edaphic media), and 0.50 m and 1.50 m layers (belonging to underlying media) below the surface. Soil adapters for horizontal positioning made of a PTFE filter were installed with the soil CO_2 sensor (215519, Vaisala, Inc., Finland) for water protection. The CO_2 sensors were configured to measure the CO_2 molar fractions at a temperature of 25 °C and 1013 hPa, but during the post-processing measurements were corrected for soil temperature and pressure at the time of measurements. Data were recorded every 30 s and stored as 30 min averages in a data-logger (CR23X and CR1000, Campbell Scientific, Logan, UT, USA; respectively for AM and BB). Missing data vary 3–6% over the entire period (2014–2016) except in AM for χ_c at 1.50 m (22%), and in BB for soil temperature at 1.50 m (48%) and χ_c at 0.50 m (50%) due to instrument malfunction.

At both experimental sites, meteorological measurements of atmospheric pressure (p ; open-path infrared gas analyzer Li-Cor 7500, Lincoln, NE, USA), wind speed (CSAT-3, Campbell Scientific, Logan, UT, USA), net radiation (NR Lite, Kipp&Zonen, Delft, Netherlands), air temperature and air relative humidity (HMP35-C,

Campbell Scientific, Logan, UT, USA) and rainfall (745 M, Davis Instruments Corp., Hayward, CA, USA) were acquired since 2009. Meteorological data were recorded as 30 min averages by a data logger (CR3000, Campbell Scientific, Logan, UT, USA). Missing data for all meteorological variables in both sites corresponded to <10% over the entire period. For more information about the site and meteorological equipment see López-Ballesteros et al. (2018).

2.3. Data Analysis

Outliers were detected with a 2.5-hour sliding standard deviation window across neighboring values. Small gaps (less than a week) were filled by estimating extrapolated values from forward and reverse autoregressive fits of the remaining samples. Gaps of more than a week were filled with a simple regression fit with the same soil depth profile from the other experimental site, (except for CO₂ at 0.50 m in BB where correlation was higher with CO₂ at 1.50 m in AMO, $R^2 > 0.5$). Atmospheric pressure gaps were filled using a simple regression with measurements from the other experimental site ($R^2 > 0.96$). In order to analyze the relationship between differences at 30 min averages in T_{soil} and subsoil χ_c variations, both simple regression and Spearman partial correlation analyses were performed considering the effect of T_{soil} or VWC. In order to study the time series at the seasonal scale, we distinguish in the database between growing or wet (March–April) and dry (July–August) season. The periods selected are periods in which “dry” and “wet” conditions occurs in each year analyzed.

We used the continuous wavelet transform to describe the temporal variability, explore the spectral properties and investigate the temporal correlations (Cazelles et al., 2008; Govindan et al., 2005; Grinsted et al., 2004; Torrence & Compo, 1998) between χ_c and p , T_{soil} and VWC during three years. Wavelet coherence analysis (WCA) is useful to identify significant temporal correlations between two time series (Grinsted et al., 2004). We calculated the WCA between χ_c and p and the soil variables (T_{soil} and VWC) with statistical significance ($p < 0.05$) using 1000 Monte Carlo simulations. As a mother function, we used the Morlet wavelet, which is a widely used non-orthogonal wavelet for time and scale resolution (Torrence & Compo, 1998). All time series were analyzed using a 1-hour time step. WCA ranges between 0 and 1, where 1 indicates the highest temporal correlation (and 0 for no correlation) between variables. Yellow areas with black contour lines represent a high significant temporal correlation with 5% significance level. In addition, arrows show the phase-locked angle relationship between both time series (Govindan et al., 2005; Grinsted et al., 2004; Xu et al., 2014). The WCA has been previously used for continuous measurements of soil carbon dynamics (Vargas et al., 2012, 2018; Xu et al., 2014). All data analyses were performed using MATLAB R2017a (MathWorks, Natick, Massachusetts, USA).

3. Results

3.1. Environmental Conditions

The annual mean air temperature during the study period was 18.5 ± 5.9 °C in AM and 17.7 ± 6.4 °C in BB. The warmest summer and winter were in 2015 and 2016, respectively. Both ecosystems show the same rainfall pattern although BB always had a slightly higher precipitation regime (15%). The driest year was 2014 with 134 mm in AM and 166 mm in BB, with lower precipitation than the typical precipitation regime established in the area (220 mm). In contrast, 2015 and 2016 were rainy years with 201 mm and 264 mm respectively in AM and 237 mm and 284 mm in BB.

Seasonal and annual patterns of atmospheric pressure (p), volumetric water content (VWC), soil temperature (T_{soil}) and precipitation are shown for both experimental sites in Figure 2. Fluctuations in p were similar in BB and AM. There was a seasonal pattern in the range of variation, with winter months having the highest maximum and minimum values. Regarding T_{soil} , both ecosystems showed similar values. Maxima and minima were reached in the shallower layer (0.15 m) with values ranging between 9 °C and 34 °C in AM, versus 5 °C and 35 °C in BB. With a slight decrease in the amplitude of daily fluctuations in comparison with the shallower layer, T_{soil} was very similar at 0.50 m in both ecosystems. At 1.50 m the lowest range of variation was observed and the maximum and minimum values were reached with a ~20 days delay in relation with the shallowest layer. At this depth maximum T_{soil} was reached in August (~27 °C) while minimum was reached in February (~18 °C). Finally, the annual mean VWC was $7.5 \pm 2.6\%$ in AM and $8.7 \pm 2.9\%$ in BB with minima around 5–6% in AM and 3–4% in BB and maxima of 42% in AM and 50% in BB

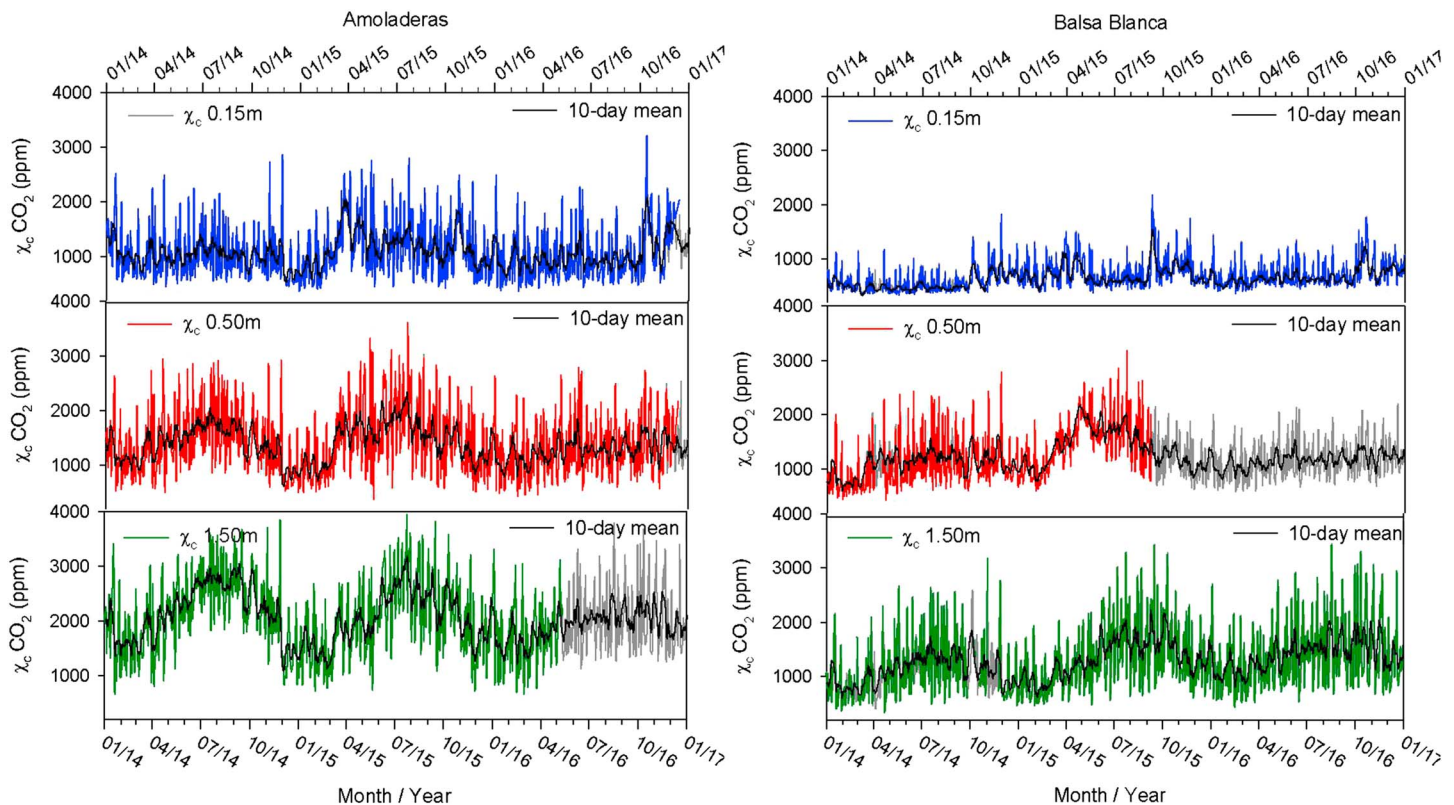


Figure 3. Daily-averaged (solid lines) and 10-day mean (dotted lines) values of soil CO₂ molar fraction (χ_c) at 0.15 m, 0.50 m and 1.50 m depth during the study period (January 2014–December 2016). Shaded lines represent gaps in the time series.

coinciding with local storms. After these storms, the VWC in AM returned rapidly to its base level in comparison with a longer recovery in VWC for BB.

3.2. Dynamics of Soil CO₂ Molar Fractions at Different Temporal Scales

Soil CO₂ showed a clear vertical profile with higher concentration at depth, and similar means over the three years (Figure 3). The year with the highest χ_c was 2015 (with an annual average across the multiple soil depths of 1558 ± 429 ppm in AM and 1161 ± 329 ppm in BB). The χ_c showed clear annual patterns with maxima in summer and minima in winter. Generally, AM had higher CO₂ concentrations across the multiple soil depths. For example, χ_c at 1.50 m had an annual average of 2029 ± 113 ppm in AM and 1268 ± 154 ppm in BB. AM also showed higher variability, particularly at 0.15 m (Figure 3).

During the whole study period, we detected sub-daily and synoptic patterns in p and χ_c , even during the first precipitation events at the end of the dry season, with inverse correlation between both variables (Table 1; Figure 4). At the synoptic scale (oscillation in p induced by the passage of high and low pressure systems and fronts), p changes lasted from 3 to 8 days approximately. However, at daily scale there were two cycles per day, and the first generally had a lower amplitude than the second. Regarding χ_c , daily fluctuations up to 2000 ppm CO₂ occurred during periods of less than 6 hours (c.f. 19 September 2014; Figure 4). At all depths, χ_c was generally higher in AM (Figures 3 and 4). On the other hand, χ_c showed similar values at 0.50 m and 1.50 m in BB (Figure 4), while in AM an increment in χ_c with depth was more evident.

3.3. The Effect of Atmospheric Pressure on CO₂ Molar Fraction Fluctuations

We found strong significant partial correlations between variations in atmospheric p and variations in χ_c ($p < 0.01$; Table 1). This correlation was not influenced by the indirect effect of T_{soil} or VWC, and was always higher at AM. In general, the degree of correlation increased with depth reaching correlation coefficients of -0.79 in AM for wet season and -0.70 in BB at 1.50 m for dry season. We also found seasonal differences,

Table 1

Correlation Coefficients (r) of Spearman Partial Correlation Between Variations in Atmospheric Pressure (Δp) and Variations in Soil CO_2 Molar Fraction ($\Delta\chi_c$) at Three Depths (0.15 m, 0.50 m and 1.50 m) in Half-hour Values During the Study Period (Year; January 2014–December 2016), Considering Growing Wet (Wet; March–April) and Dry Season (Dry; July–August)

Amoladeras		Δp	$\Delta p(\Delta T_{\text{soil}})$	$\Delta p(\Delta \text{VWC})$	$\Delta p(\Delta T_{\text{soil}}, \Delta \text{VWC})$
$\Delta\chi_c$ 0.15m	year	-0.59	-0.55	-0.54	-0.54
	dry	-0.67	-0.62	-0.66	-0.62
	wet	-0.58	-0.54	-0.58	-0.53
$\Delta\chi_c$ 0.50m	year	-0.75	-0.75	-0.75	-0.75
	dry	-0.76	-0.76	-0.76	-0.76
	wet	-0.78	-0.78	-0.78	-0.78
$\Delta\chi_c$ 1.50m	year	-0.75	-0.75	-0.74	-0.74
	dry	-0.71	-0.71	-0.70	-0.70
	wet	-0.79	-0.79	-0.79	-0.79
Balsa Blanca		Δp	$\Delta p(\Delta T_{\text{soil}})$	$\Delta p(\Delta \text{VWC})$	$\Delta p(\Delta T_{\text{soil}}, \Delta \text{VWC})$
$\Delta\chi_c$ 0.15m	year	-0.41	-0.31	-0.40	-0.31
	dry	-0.45	-0.35	-0.40	-0.34
	wet	-0.40	-0.29	-0.39	-0.29
$\Delta\chi_c$ 0.50m	year	-0.43	-0.43	-0.43	-0.43
	dry	-0.66	-0.63	-0.63	-0.63
	wet	-0.28	-0.28	-0.28	-0.28
$\Delta\chi_c$ 1.50m	year	-0.62	-0.64	-0.61	-0.62
	dry	-0.70	-0.72	-0.70	-0.69
	wet	-0.62	-0.65	-0.62	-0.63

Note. Indirect effect of variations in soil temperature (ΔT_{soil}) at three depths (0.15 m, 0.50 m and 1.50 m), variations in volumetric water content (ΔVWC) at 0.50 m, and the combined effect of soil temperature and volumetric water content ($\Delta T_{\text{soil}}, \Delta \text{VWC}$) are controlled in their respective columns. Filled data are not considered for this analysis (sample size, $n \geq 8784$; all the coefficients had p -value < 0.01).

with more correlation in the shallower layer (0.15 m) during the dry season in both sites, whereas the growing season presented the highest partial correlation at 1.50 m and 0.50 m in AM. The weakest correlation was found at 0.50 m in BB (-0.28 during the wet season; $p < 0.01$; Table 1).

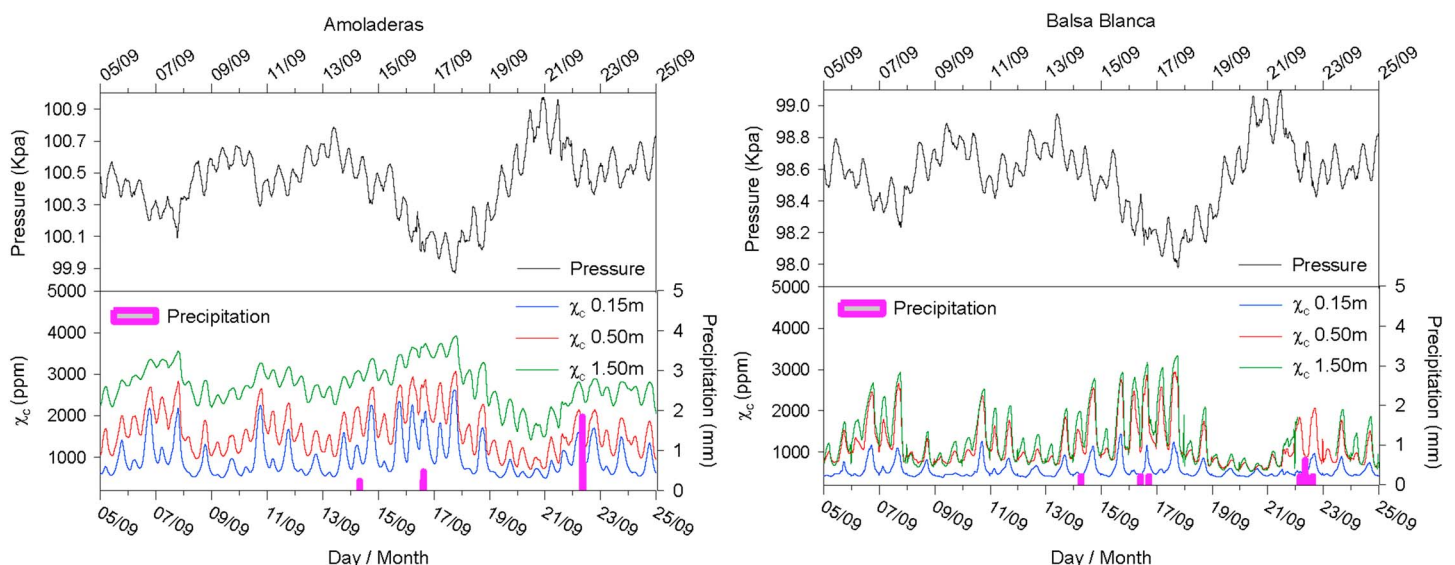


Figure 4. Average half-hour values of atmospheric pressure and soil CO_2 molar fraction (χ_c) at 0.15 m, 0.50 m and 1.50 m depths during the period 05–25 September of 2014.

3.4. Wavelet Coherence Analysis

We used wavelet coherence analysis (WCA) to test the temporal correlation between χ_c and ancillary variables. The yellow areas inside the contour lines represent high local temporal correlation between both series (Figures 5, 6 and 7). This analysis showed that p had a strong temporal correlation with χ_c in the deep soil (Figure 5), much higher than T_{soil} (Figure 6) or VWC (Figure 7). The WCA also indicated the main periodic components in the frequency domain between time series, showing a strong spectral coherence between variations of p and changes in χ_c (Figure 5), at periodicities ranging from 0.5 day to ~30 days (shown as yellow areas with black contour lines during this period) throughout the study period. Finally, the almost horizontal arrows pointing left indicated that oscillations were out of phase (Figure 5). This means that increments in χ_c corresponded to decreases in p and *viceversa*, at these temporal scales. This interpretation was consistent with the temporal pattern visible in Figure 4 and Table 1, which showed semidaily, daily and a synoptic patterns of variation, while the quasi-monthly pressure-CO₂ fluctuation was not evident from the WCA.

The WCA showed strong spectral coherence between variations of T_{soil} or VWC and changes in χ_c (Figures 6 and 7) at daily and annual scale (shown as yellow areas with black contour lines at 1 day and 256 days) at 0.15 m. Contrary to the p - χ_c relationship, there was a high seasonality in this correlation in the case of T_{soil} in BB and in both ecosystems with VWC, with both variables particularly correlated during dry season. The causality relation – with T_{soil} or VWC forcing variations in χ_c – diminished with depth.

4. Discussion

Changes in atmospheric pressure (p) conditions induce the expansion or contraction of the air stored in soil pores within the vadose zone, which plays a dominant role in regulating CO₂ storage and vertical transport. Simple regressions, Spearman partial correlations and spectral analysis consistently showed that CO₂ dynamics strongly depend on changes in atmospheric pressure (Figures 4, 5 and Table 1). We propose that the underlying physical mechanism is related to pressure tides (Kuang et al., 2013; Le Blancq, 2011; Lindzen, 1979; Massmann & Farrier, 1992). Pressure fluctuations penetrate deep into the soil vertical profile with very little attenuation (Maier et al., 2010; Massmann & Farrier, 1992; Takle et al., 2004), and the soil air expands upward in conditions of falling p or is compressed downward under rising p (Redeker et al., 2015; Sánchez Cañete, Kowalski, et al., 2013), which may induce a natural “soil breathing phenomenon”. The p influence was stronger in the deepest layer (Table 1 and Figure 5), where χ_c was higher and there was a lower influence of soil temperature (T_{soil}) and volumetric water content (VWC). Petrophysical properties of soil medium, such as permeability and connectivity, are pivotal factors in the p influence. These factors differs between layers producing discontinuities (Zamanian et al., 2016) that can slow down or facilitate the circulation of soil gases.

According to wavelet coherence analysis (WCA), the temporal correlation between p and χ_c (Figure 5) presented strong variations at different time scales. The dominant periods range from 0.5 day to ~30 days, implicating clear semidiurnal, diurnal, synoptic (Figure 4) and monthly temporal coherence (Figure 5). At semi-daily and daily scale in our experimental sites, the pressure tides showed two peaks per day, and generally, the first peak was smaller than the second (Figure 4). This bimodal pattern was produced in the opposite way in the χ_c , with daily fluctuations up to 2000 ppm during intervals of less than 6 hours (Figure 4). Semi-daily and daily fluctuations in CO₂ dynamics have been related with gravitational forcing produced by sun and the moon (Lindzen, 1979; Sánchez Cañete, Kowalski, et al., 2013), and are mainly forced by daily variations in insolation due to diurnal heating of Earth’s surface (Kimball & Lemon, 1970; Le Blancq, 2011). At the synoptic scale, the pressure tide effect was also detected. This pattern of variation ranged between 3 and 8 days (Figure 4) induced by synoptic weather changes (the passage of high and low pressure systems and fronts; Clements & Wilkening, 1974; Elberling et al., 1998; Sánchez Cañete, Kowalski, et al., 2013). With respect to the monthly scale, we are not aware of any other studies relating CO₂ dynamics to pressure tides. However, the WCA showed a clear quasi-monthly pressure-CO₂ fluctuation that was visible during the three years of the experiment at both experimental sites (Figure 5). At this temporal scale, lunar forcing is the predominant factor affecting atmospheric tides with a 27.3-day and 13.6-day atmospheric oscillation affected by the lunar declination and the lunar revolution around the Earth (Guoqing, 2005).

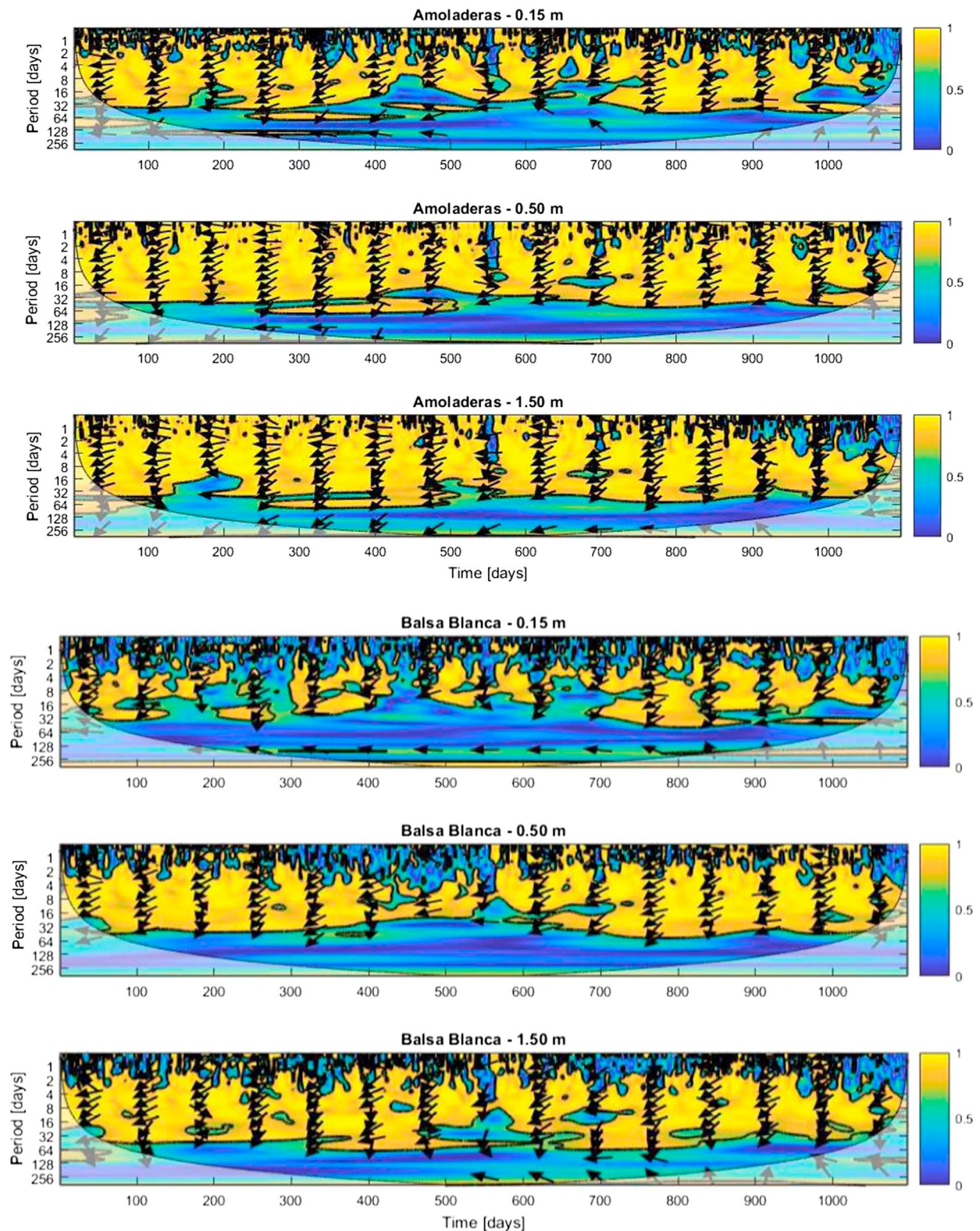


Figure 5. Average 1-hour wavelet coherence analysis (WCA) to test the influence of atmospheric pressure on soil CO₂ molar fraction at three depths (0.15 m, 0.50 m and 1.50 m) in Amoladeras and Balsa Blanca experimental sites. Yellow areas with black contour lines represent a high significant temporal correlation with 5% significance level. Shaded area represents the cone of influence, where correlation is not influenced by edge effects. Arrows show the phase-locked angle relationship between the two time series. Horizontal arrows pointing right (phase angle of 0°) indicate that the two time series are in phase, and horizontal arrows pointing left (phase angle of 180°) represent when the two time series are out of phase.

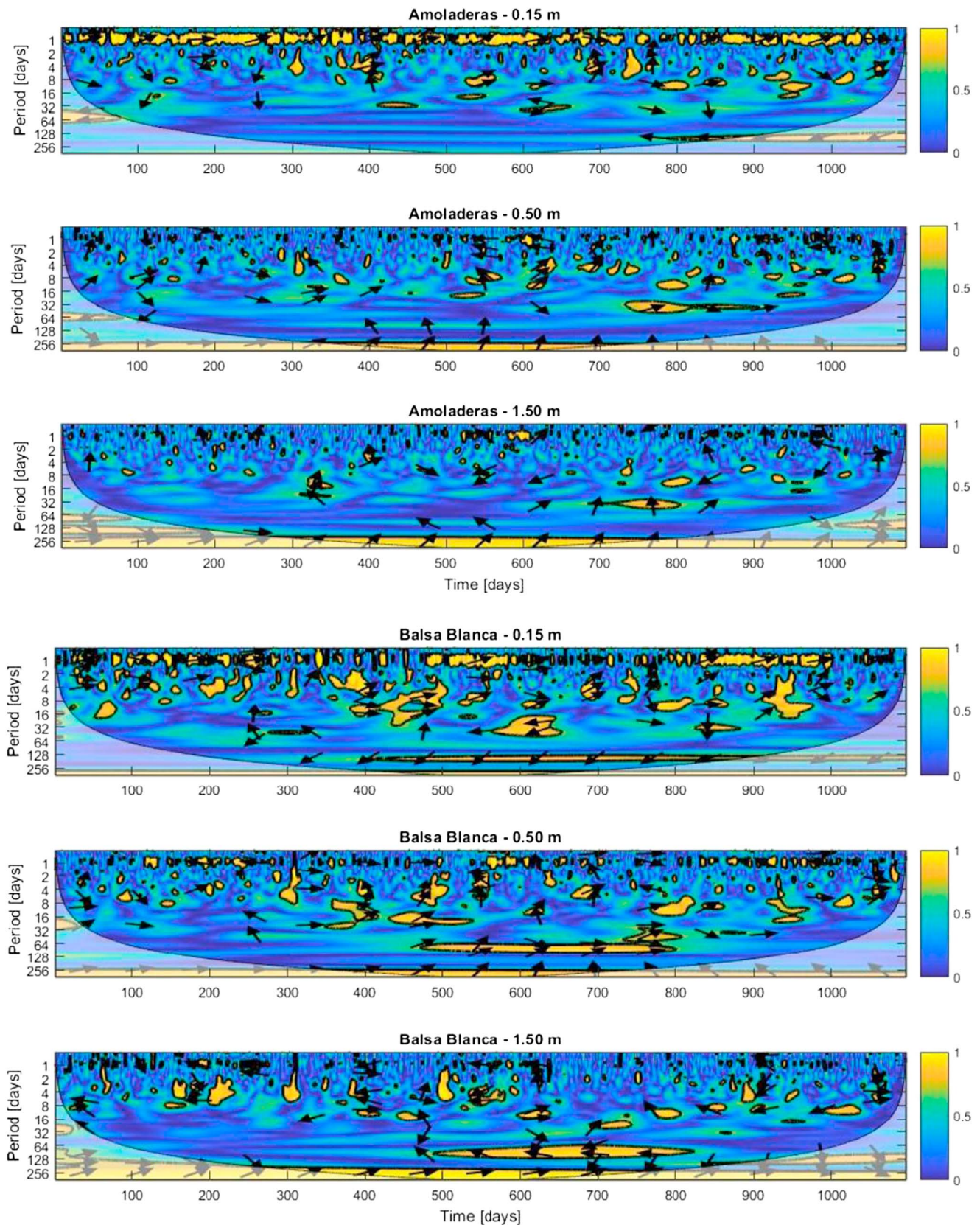


Figure 6. Average 1-hour wavelet coherence analysis (WCA) to test the influence of soil temperature on soil CO_2 molar fraction at three depths (0.15 m, 0.50 m and 1.50 m) in Amoladeras and Balsa Blanca experimental sites. Information about the interpretation of this figure can be found in the caption for Figure 5.

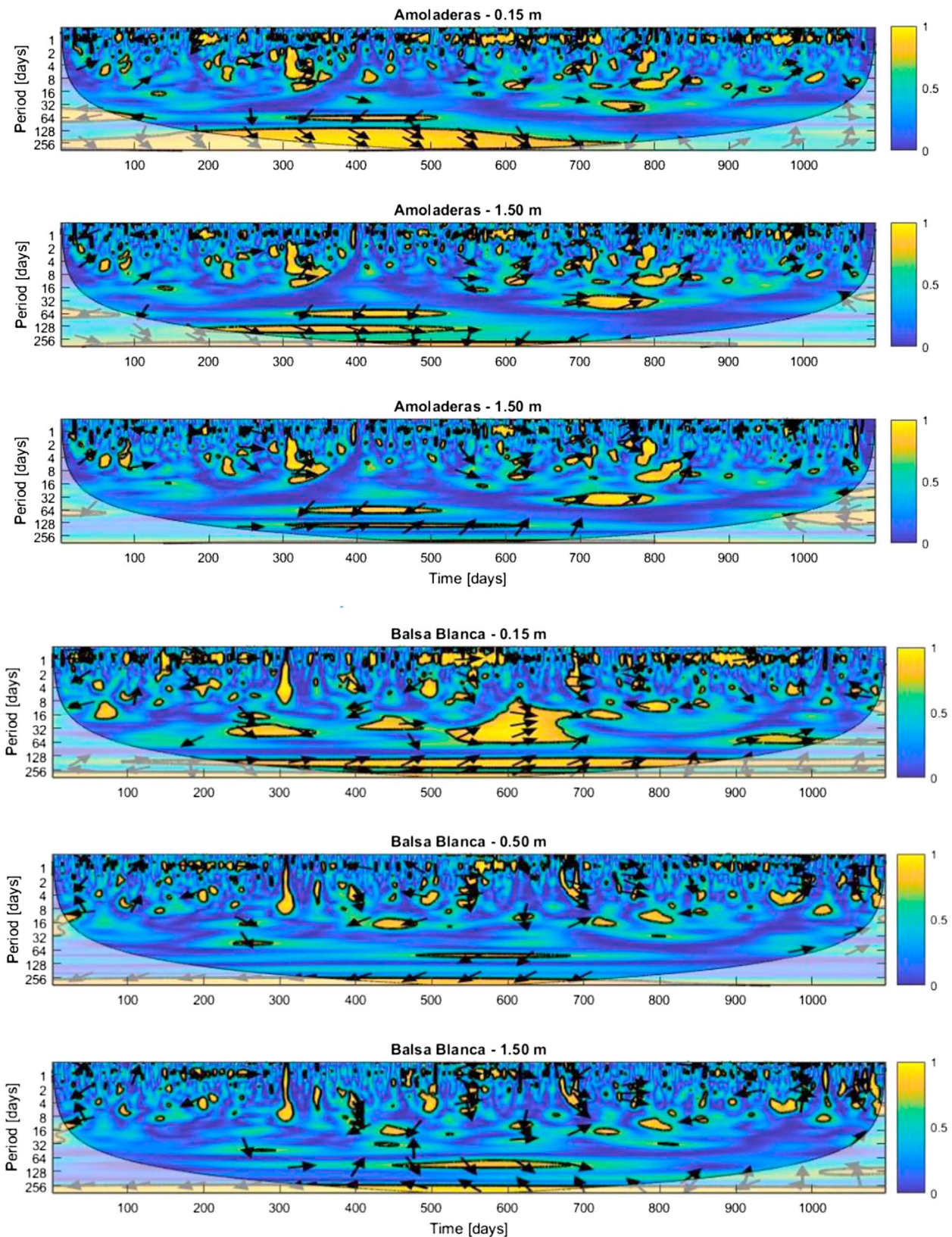


Figure 7. Average 1-hour wavelet coherence analysis (WCA) to test the influence of volumetric water content at 0.50 m on soil CO₂ molar fraction at three depths (0.15 m, 0.50 m and 1.50 m) in Amoladeras and Balsa Blanca experimental sites. Information about the interpretation of this figure can be found in the caption of Figure 5.

At high-frequencies (< 1 Hz; Massman et al., 1997; Mohr et al., 2016; Roland et al., 2015), the friction velocity (indicator of turbulence) drives p fluctuations (Maier et al., 2010; Redeker et al., 2015). There is no clear distinction between pressure pumping and ventilation, a physical phenomena produced by turbulence that is associated with abrupt emissions of CO_2 to the atmosphere via non diffusive transport presented in well-aerated soils (Kowalski et al., 2008; Sanchez-Cañete et al., 2011). Some authors have stated a positive relationship between both processes (Mohr et al., 2016; Nachshon et al., 2012; Redeker et al., 2015), considering a correlation between p changes and wind perturbations. A low correlation between pressure tides and wind velocity was detected in BB only at 0.15 m (similar to results obtained by Sánchez Cañete, Kowalski, et al., 2013) and no correlation was detected in the deep profile in AM (data not shown). Although the high-frequency pressure oscillation and wind turbulence are not measured in this study, ventilation events had been detected in the past in the experimental sites of Balsa Blanca (BB; Rey et al., 2012) and Amoladeras (AM; López Ballesteros et al., 2017), with AM having the higher ventilation potential (López-Ballesteros et al., 2018). Unlike pressure tides, high-frequency pressure fluctuations caused by winds are known to undergo strong attenuation with soil depth (Redeker et al., 2015; Takle et al., 2004). This different capacity of permeability could create a possible decoupling between the shallower horizons, affected by ventilation, pressure pumping and pressure tides; and deeper layers, that would be affected only by pressure tides. This assumption could explain the lack of relationship found between wind turbulence and p changes in BB and AM in the vertical profile, even though ventilation events have been detected at the ecosystem scale (López Ballesteros et al., 2017; Rey et al., 2012).

Proximity to the coast (3.6 Km in AM and 6.3 Km in BB) could influence the atmospheric pressure tide effect on soil χ_c and explain the higher range of variation in the χ_c in AM, as well as the higher pressure tidal effect in comparison with BB (Figures 3 and 4). The water table provides a low-permeable boundary between the vadose zone and the soil surface that in coastal areas fluctuates frequently in response to sea tidal variations (Jiao & Tang, 1999; Li & Barry, 2000). At our experimental sites the water table is at 50 m depth approximately (Junta de Andalucía, C. d. M. A. y. O. d. T, 2013). Fluctuations in the water table changes the volume of the vadose zone; changing the depth of air penetration (Jiao & Li, 2004; Maier et al., 2010). When the water table rises, air is forced to be compressed in the vadose zone generating positive pressures and therefore, the air stored in the pores and fissures could be pushed up to shallower layers. On the contrary, when the water table falls, extra pore space and negative pressures are generated (Jiao & Li, 2004). Dong et al. (2014) studied a coastal aquifer near the Ariake Sea, where the groundwater level of the coastal aquifer fluctuated with tidal and barometric variations. Here, spectral analyses also revealed that the sea-tidal effects could influence the semi-monthly, diurnal, and semidiurnal periodicities, associated with the astronomical tidal variations.

Other differences between study sites may be relevant. Firstly, due to its geographical position in the subterranean aquifer system (Junta de Andalucía, C. d. M. A. y. O. d. T, 2013), AM would have a higher allochthonous CO_2 recharge than BB explaining its higher χ_c concentration (Figures 3 and 4; López Ballesteros et al., 2017). Secondly, the higher fraction of bare soil and rocks, the differing content in SOC, lower microbial activity or thinner soil depth are “degradation indicators” exhibited by AM (López-Ballesteros et al., 2018; Rey et al., 2011). These indicators suggest an increase in the interconnectivity between the soil medium and the atmosphere, and could enhance the gas transport and storage capacity of the medium, producing changes at the surface (López-Ballesteros et al., 2018). This would explain why in AM χ_c is more influenced by p changes (driver of physical transport processes in the χ_c dynamics) than in BB (Figure 5), while the influence of VWC and T_{soil} (drivers of biological processes in the χ_c dynamics) is higher in BB and only relevant at 0.15 m depth (Figures 6, 7). Thirdly, in AM the VWC at 0.50 m returns to its base level rapidly after a local storm, while in BB it takes longer for VWC to return to pre-storm levels (Figure 2). This suggests that the soil in AM favors drainage and is more porous than in BB, enhancing CO_2 storage and vertical transport.

Seasonal differences were also found in both ecosystems. During the dry season, coinciding with the maximum water-free pore space, when the aeration between soil and atmosphere is higher (Cuezva et al., 2011; Loisy et al., 2013), a higher correlation between χ_c and p was found in the shallower layer (Table 1). Spectral analysis also showed a marked seasonal pattern in the temporal correlations between variations of χ_c and changes in VWC (in BB and AM; Figure 7) and T_{soil} (in BB; Figure 6) in the shallowest layer (0.15 m), which are higher during dry season.

Most studies interpret the soil CO₂ efflux as instantaneous soil respiration and the more basic models are built by using soil temperature and soil water content relationships (Almagro et al., 2009; Davidson et al., 1998). However, at our experimental sites, T_{soil} and VWC are only relevant at 0.15 m for soil χ_c dynamics. Instead, changes in atmospheric pressure is the main driver in the deep soil profile (Figures 5, 6 and 7). Similar effects were detected in different ecosystems by some studies that estimated a temporary transport enhancement by pressure pumping (Bowling & Massman, 2011; Maier et al., 2012; Takle et al., 2004). However, there are no similar studies analyzing pressure tides and their relation with CO₂ fluxes at low frequencies (> 1 Hz). Although the air flux induced by pressure fluctuation is only effective for a limited period (Maier et al., 2010), the omission of non-diffusive processes in the flux-gradient approach (Fick's law), generates an underestimation of the real CO₂ efflux rates and its transport in soil that casts doubt on its assumptions. Therefore, we propose that it is important to consider this effect when the soil gas flux is determined using the gradient method, at least, in ecosystems with high interconnectivity between the unsaturated porous media and the atmosphere (Fang & Moncrieff, 1999; Redeker et al., 2015; Vargas et al., 2010). There have been several attempts to incorporate this physical phenomenon. Based on empirical modeling, Mohr et al. (2016) defined a pressure pumping coefficient that would be able to describe the strength of the pressure-pumping effect on injected helium. Goffin et al. (2015) created an alternative model considering air pressure fluctuations at the soil surface with the air permeability to calculate the soil CO₂ efflux. They concluded that the influence of pressure fluctuations creates a higher instantaneous flux compared to the diffusive flux only observable on very short timescales. Finally, Xu et al. (2014) created a model where the volume of CH₄ transported through porous media was correlated with a pressure change rate. These approaches could serve as bases to improve the gradient method in ecosystems affected by non-diffusive gas transport processes (Maier et al., 2012; Webb & Pruess, 2003).

5. Conclusions

This study assessed the main factors controlling soil CO₂ dynamics in the vadose zone of two semi-arid grasslands at different soil depths and time-scales. Our results showed that CO₂ dynamics at two semi-arid grasslands strongly depend on changes in atmospheric pressure. This dependency was consistent across soil depths, time-scales and study periods. We found strong evidence of non-diffusive CO₂ transport at our sites, with fluctuations of up to 2000 ppm CO₂ in less than 6 hours driven by pressure tides at scales ranging from 0.5 to ~30 days, showing semidiurnal, diurnal, synoptic and monthly patterns of oscillation. The atmospheric pressure effect on the soil CO₂ concentration was more evident in deeper layers, during the dry season and in the more degraded ecosystem. Pressure fluctuations penetrated deep into the soil vertical profile with very little attenuation, suggesting a bulk transport mechanism of trace gases throughout the porous medium that is much more effective than diffusion. This approach showed the importance of subterranean storage and non-diffusive gas transport and suggested the need to consider non-diffusive gas transport processes in models. The improvement of the gradient method (beyond Fick's law) will be essential for reliable estimations of the soil CO₂ efflux in ecosystems affected by non-diffusive gas transport processes.

References

- Ahlström, A., Raupach, M. R., Schurgers, G., Smith, B., Arneth, A., Jung, M., et al. (2015). The Dominant Role of Semi-Arid Ecosystems in the Trend and Variability of the Land CO₂ Sink. *Science*, 348(6237), 895–899. <https://doi.org/10.1126/science.aaa1668>
- Alados, C. L., Pueyo, Y., Barrantes, O., Escós, J., Giner, L., & Robles, A. B. (2004). Variations in landscape patterns and vegetation cover between 1957 and 1994 in a semiarid Mediterranean ecosystem. *Landscape Ecology*, 19(5), 543–559. <https://doi.org/10.1023/B:LAND.0000036149.96664.9a>
- Almagro, M., López, J., Querejeta, J. I., & Martínez-Mena, M. (2009). Temperature dependence of soil CO₂ efflux is strongly modulated by seasonal patterns of moisture availability in a Mediterranean ecosystem. *Soil Biology and Biochemistry*, 41(3), 594–605. <https://doi.org/10.1016/j.soilbio.2008.12.021>
- Baldini, J. U. L., Baldini, L. M., McDermott, F., & Clipson, N. (2006). Carbon dioxide sources, sinks, and spatial variability in shallow temperate zone caves: Evidence from Ballynamintra cave, Ireland. *Journal of Cave and Karst Studies*, 68(1), 4–11.
- Benavente, J., Vadillo, I., Carrasco, F., Soler, A., Liñán, C., & Moral, F. (2010). Air carbon dioxide contents in the vadose zone of a mediterranean karst. *Vadose Zone Journal*, 9(1), 126–136. <https://doi.org/10.2136/vzj2009.0027>
- Bowling, D. R., & Massman, W. J. (2011). Persistent wind-induced enhancement of diffusive CO₂ transport in a mountain forest snowpack. *Journal of Geophysical Research*, 116, G04006. <https://doi.org/10.1029/2011JG001722>
- Buyanovsky, G. A., & Wagner, G. H. (1983). Annual cycles of carbon dioxide level in soil air. *Soil Science Society of America Journal*, 47(6), 1139–1145. <https://doi.org/10.2136/sssaj1983.03615995004700060016x>
- Cazelles, B., Chavez, M., Berteaux, D., Ménard, F., Vik, J. O., Jenouvrier, S., & Stenseth, N. C. (2008). Wavelet analysis of ecological time series. *Oecologia*, 156(2), 287–304. <https://doi.org/10.1007/s00442-008-0993-2>

Acknowledgments

María Rosario Moya Jiménez acknowledges support from the Ministry of Education, Culture and Sport (FPU grant, 14/03497). This research was funded in part by the Spanish Ministry of Economy and Competitiveness projects GEISpain (CGL2014-52838-C2-2-R) and DINCOS (CGL2016-78075-P), including European Union ERDF funds, CARBOLIVAR (CGL2014-52838-C2-1-R) funded by the Consejería de Innovación, Ciencia y Empresa de la Junta de Andalucía, and the 7th European Community Framework Programme, DIESEL project (N° 625988). RV acknowledges support from the National Science Foundation (#1652594), and from the University of Almería and the Experimental Station of Arid Zones to visit the study site. The program “Unidades de Excelencia Científica del Plan Propio de Investigación de la Universidad de Granada” funded the cost of this publication. The authors are grateful to Enrique Cortés, Alfredo Durán, Domingo Álvarez and Ángel Belmonte for the maintenance of the field measurement devices. The authors wish to thank also to the anonymous reviewers for their constructive comments. All data used in this study are freely available at <https://doi.org/10.6084/m9.figshare.7381580.v2>.

- Clements, W. E., & Wilkening, M. H. (1974). Atmospheric pressure effects on ^{222}Rn transport across the Earth-air interface. *Journal of Geophysical Research*, 79(33), 5025–5029. <https://doi.org/10.1029/JC079i033p05025>
- Corey, A. T., Kemper, W. D., & Dane, J. H. (2010). Revised model for molecular diffusion and advection. *Vadose Zone Journal*, 9(1), 85–94. <https://doi.org/10.2136/vzj2009.0082>
- Cuezva, S., Fernandez-Cortes, A., Benavente, D., Serrano-Ortiz, P., Kowalski, A. S., & Sanchez-Moral, S. (2011). Short-term CO_2 exchange between a shallow karstic cavity and the external atmosphere during summer: Role of the surface soil layer. *Atmospheric Environment*, 45(7), 1418–1427. <https://doi.org/10.1016/j.atmosenv.2010.12.023>
- Davidson, E. A., Belk, E., & Boone, R. D. (1998). Soil water content and temperature as independent or confounded factors controlling soil respiration in a temperate mixed hardwood forest. *Global Change Biology*, 4(2), 217–227. <https://doi.org/10.1046/j.1365-2486.1998.00128.x>
- Denis, A., Lastennet, R., Huneau, F., & Malaurent, P. (2005). Identification of functional relationships between atmospheric pressure and CO_2 in the cave of Lascaux using the concept of entropy of curves. *Geophysical Research Letters*, 32, L05810. <https://doi.org/10.1029/2004GL022226>
- Dong, L., Shimada, J., Kagabu, M., & Yang, H. (2014). Barometric and tidal-induced aquifer water level fluctuation near the Ariake Sea. *Environmental Monitoring and Assessment*, 187(1), 4187. <https://doi.org/10.1007/s10661-014-4187-6>
- Duniway, M. C., Herrick, J. E., & Monger, C. (2007). The High Water-Holding Capacity of Petrocalcic Horizons. *Soil Science Society of America Journal*, 71(3). <https://doi.org/10.2136/sssaj2006.0267>
- Elberling, B., Larsen, F., Christensen, S., & Postma, D. (1998). Gas transport in a confined unsaturated zone during atmospheric pressure cycles. *Water Resources Research*, 34(11), 2855–2862. <https://doi.org/10.1029/98WR02037>
- Fang, C., & Moncrieff, J. B. (1999). A model for soil CO_2 production and transport 1: Model development. *Agricultural and Forest Meteorology*, 95(4), 225–236. [https://doi.org/10.1016/S0168-1923\(99\)00036-2](https://doi.org/10.1016/S0168-1923(99)00036-2)
- FAO (2009). *Guía para la Descripción de Suelos* (4ª edición ed., p. 99). Roma, Italia.
- García-Anton, E., Cuezva, S., Fernández-Cortes, A., Benavente, D., & Sánchez-Moral, S. (2014). Main drivers of diffusive and advective processes of CO_2 -gas exchange between a shallow vadose zone and the atmosphere. *International Journal of Greenhouse Gas Control*, 21, 113–129. <https://doi.org/10.1016/j.ijggc.2013.12.006>
- Goffin, S., Wylock, C., Haut, B., Maier, M., Longdoz, B., & Aubinet, M. (2015). Modeling soil CO_2 production and transport to investigate the intra-day variability of surface efflux and soil CO_2 concentration measurements in a Scots Pine Forest (*Pinus sylvestris*, L.). *Plant and Soil*, 390(1–2), 195–211. <https://doi.org/10.1007/s11104-015-2381-0>
- Govindan, R. B., Raethjen, J., Kopper, F., Claussen, J. C., & Deuschl, G. (2005). Estimation of time delay by coherence analysis. *Physica A: Statistical Mechanics and its Applications*, 350(2), 277–295. <https://doi.org/10.1016/j.physa.2004.11.043>
- Grinsted, A., Moore, J. C., & Jevrejeva, S. (2004). Application of cross wavelet transform and wavelet coherence to geophysical time series. *Nonlinear Processes in Geophysics*, 11, 561–566. <https://doi.org/10.5194/npg-11-561-2004>
- Guoqing, L. (2005). 27.3-day and 13.6-day atmospheric tide and lunar forcing on atmospheric circulation. *Advances in Atmospheric Sciences*, 22(3), 359–374. <https://doi.org/10.1007/bf02918750>
- IUSS Working Group WRB (2015). World Reference Base for soil resources 2014, update 2015 International soil classification system for naming soils and creating legends for soil maps. World Soil Resources Reports No. 106. FAO, Rome.
- Jiao, J. J., & Li, H. (2004). Breathing of coastal vadose zone induced by sea level fluctuations. *Geophysical Research Letters*, 31, L11502. <https://doi.org/10.1029/2004GL019572>
- Jiao, J. J., & Tang, Z. (1999). An analytical solution of groundwater response to tidal fluctuation in a leaky confined aquifer. *Water Resources Research*, 35(3), 747–751. <https://doi.org/10.1029/1998WR900075>
- Junta de Andalucía, C. d. M. A. y. O. d. T. (2013). Mapa de información general de aguas subterráneas de Andalucía, edited, Red de Información Ambiental de Andalucía (REDIAM).
- Kimball, B. A., & Lemon, E. R. (1970). Spectra of air pressure fluctuations at the soil surface. *Journal of Geophysical Research*, 75(33), 6771–6777. <https://doi.org/10.1029/JC075i033p06771>
- Kimball, B. A., & Lemon, E. R. (1971). Air turbulence effects upon soil gas exchange. *Soil Science Society of America Journal*, 35(1), 16–21. <https://doi.org/10.2136/sssaj1971.03615995003500010013x>
- Kowalski, A. S., Serrano-Ortiz, P., Janssens, I. A., Sánchez-Moral, S., Cuezva, S., Domingo, F., et al. (2008). Can flux tower research neglect geochemical CO_2 exchange? *Agricultural and Forest Meteorology*, 148(6–7), 1045–1054. <https://doi.org/10.1016/j.agrformet.2008.02.004>
- Kuang, X., Jiao, J. J., & Li, H. (2013). Review on airflow in unsaturated zones induced by natural forcings. *Water Resources Research*, 49, 6137–6165. <https://doi.org/10.1002/wrcr.20416>
- Le Blancq, F. (2011). Diurnal Pressure Variation: The Atmospheric Tide. *Weather*, 66(11), 306–307. <https://doi.org/10.1002/wea.857>
- Li, L., & Barry, D. A. (2000). Wave-induced beach groundwater flow. *Advances in Water Resources*, 23(4), 325–337. [https://doi.org/10.1016/S0309-1708\(99\)00032-9](https://doi.org/10.1016/S0309-1708(99)00032-9)
- Lindzen, R. S. (1979). Atmospheric tides. *Annual Review of Earth and Planetary Sciences*, 7(1), 199–225. <https://doi.org/10.1146/annurev.ea.07.050179.001215>
- Loisy, C., Cohen, G., Laveuf, C., Le Roux, O., Delaplace, P., Magnier, C., et al. (2013). The CO_2 -Vadose Project: Dynamics of the Natural CO_2 in a Carbonate Vadose Zone. *International Journal of Greenhouse Gas Control*, 14, 97–112. <https://doi.org/10.1016/j.ijggc.2012.12.017>
- López Ballesteros, A., Ortiz, P. S., Cañete, E. P. S., Oyonarte, C., Kowalski, A. S., Priego, Ó. P., & Domingo, F. (2016). Enhancement of the net CO_2 release of a semiarid grassland in SE Spain by rain pulses. *Journal of Geophysical Research: Biogeosciences*, 121, 52–66. <https://doi.org/10.1002/2015JG003091>
- López Ballesteros, A., Serrano Ortiz, P., Kowalski, A. S., Sánchez Cañete, E. P., Scott, R., & Domingo, F. (2017). Subterranean ventilation of allochthonous CO_2 governs net CO_2 exchange in a semiarid Mediterranean grassland. *Agricultural and Forest Meteorology*, 234–235, 115–126. <https://doi.org/10.1016/j.agrformet.2016.12.021>
- López-Ballesteros, A., Oyonarte, C., Kowalski, A. S., Serrano-Ortiz, P., Sánchez-Cañete, E. P., Moya, M. R., & Domingo, F. (2018). Can land degradation drive differences in the C exchange of two similar semiarid ecosystems? *Biogeosciences*, 15(1), 263–278. <https://doi.org/10.5194/bg-15-263-2018>
- MAGNA (2010). Mapa Geológico de España Escala 1:50.000 (MAGNA 50). Instituto Geológico y Minero de España. Retrieved from <http://info.igme.es/cartografiadigital/geologica/Magna50.aspx> (2019, January 16).
- Maier, M., & Schack-Kirchner, H. (2014). Using the gradient method to determine soil gas flux: A review. *Agricultural and Forest Meteorology*, 192–193, 78–95. <https://doi.org/10.1016/j.agrformet.2014.03.006>

- Maier, M., Schack-Kirchner, H., Aubinet, M., Goffin, S., Longdoz, B., & Parent, F. (2012). Turbulence effect on gas transport in three contrasting forest soils. *Soil Science Society of America Journal*, 76(5), 1518–1528. <https://doi.org/10.2136/sssaj2011.0376>
- Maier, M., Schack-Kirchner, H., Hildebrand, E. E., & Holst, J. (2010). Pore-space CO₂ dynamics in a deep, well-aerated soil. *European Journal of Soil Science*, 61(6), 877–887. <https://doi.org/10.1111/j.1365-2389.2010.01287.x>
- Martinez, M. J., & Nilson, R. H. (1999). Estimates of barometric pumping of moisture through unsaturated fractured rock. *Transport in Porous Media*, 36(1), 85–119. <https://doi.org/10.1023/a:1006593628835>
- Massman, W. J., Sommerfeld, R. A., Mosier, A. R., Zeller, K. F., Hehn, T. J., & Rochelle, S. G. (1997). A model investigation of turbulence-driven pressure-pumping effects on the rate of diffusion of CO₂, N₂O, and CH₄ through layered snowpacks. *Journal of Geophysical Research*, 102(D15), 18,851–18,863. <https://doi.org/10.1029/97JD00844>
- Massmann, J., & Farrier, D. F. (1992). Effects of atmospheric pressures on gas transport in the vadose zone. *Water Resources Research*, 28(3), 777–791. <https://doi.org/10.1029/91WR02766>
- Mohr, M., Laemmel, T., Maier, M., & Schindler, D. (2016). Analysis of air pressure fluctuations and topsoil gas concentrations within a Scots pine forest. *Atmosphere*, 7(10), 125. <https://doi.org/10.3390/atmos7100125>
- Nachshon, U., Dragila, M., & Weisbrod, N. (2012). From atmospheric winds to fracture ventilation: Cause and effect. *Journal of Geophysical Research*, 117, G02016. <https://doi.org/10.1029/2011JG001898>
- Nilson, R. H., Peterson, E. W., Lie, K. H., Burkhard, N. R., & Hearst, J. R. (1991). Atmospheric pumping: A mechanism causing vertical transport of contaminated gases through fractured permeable media. *Journal of Geophysical Research*, 96(B13), 21,933–21,948. <https://doi.org/10.1029/91JB01836>
- Poulter, B., Frank, D., Ciais, P., Myneni, R. B., Andela, N., Bi, J., et al. (2014). Contribution of Semi-Arid Ecosystems to Interannual Variability of the Global Carbon Cycle. *Nature*, 509(7502), 600–603. <https://doi.org/10.1038/nature13376>
- Redeker, K. R., Baird, A. J., & Teh, Y. A. (2015). Quantifying wind and pressure effects on trace gas fluxes across the soil-atmosphere interface. *Biogeosciences*, 12(24), 7423–7434. <https://doi.org/10.5194/bg-12-7423-2015>
- Reichstein, M., Bahn, M., Ciais, P., Frank, D., Mahecha, M. D., Seneviratne, S. I., et al. (2013). Climate Extremes and the Carbon Cycle. *Nature*, 500(7462), 287–295. <https://doi.org/10.1038/nature12350>
- Rey, A., Beletti-Marchesini, L., Were, A., Serrano-ortiz, P., Etiope, G., Papale, D., et al. (2012). Wind as a Main Driver of the Net Ecosystem Carbon Balance of a Semiarid Mediterranean Steppe in the South East of Spain. *Global Change Biology*, 18(2), 539–554. <https://doi.org/10.1111/j.1365-2486.2011.02534.x>
- Rey, A., Pegoraro, E., Oyonarte, C., Were, A., Escribano, P., & Raimundo, J. (2011). Impact of land degradation on soil respiration in a steppe (*Stipa tenacissima* L.) semi-arid ecosystem in the SE of Spain. *Soil Biology and Biochemistry*, 43, 393–403. <https://doi.org/10.1016/j.soilbio.2010.11.007>
- Reynolds, J. F., Stafford Smith, D. M., Lambin, E. F., Turner II, B. L., Mortimore, M., Batterbury, S. P. J. (2007). Ecology: Global Desertification: Building a Science for Dryland Development. *Science*, 316(5826), 847–851. <https://doi.org/10.1126/science.1131634>
- Roland, M., Vicca, S., Bahn, M., Ladreiter-Knauss, T., Schmitt, M., & Janssens, I. A. (2015). Importance of nondiffusive transport for soil CO₂ efflux in a temperate mountain grassland. *Journal of Geophysical Research: Biogeosciences*, 120, 502–512. <https://doi.org/10.1002/2014JG002788>
- Rolston, D. E., & Moldrup, P. (2012). Gas transport in Soils. In Y. L. P. M. Huang & E. Malcolm (Eds.), *Handbook of Soil Science and Processes* (2nd ed., Vol. 2011, pp. 8-1–8-20). Netherlands: Springer.
- Rubel, F., & Kotteck, M. (2010). Observed and projected climate shifts 1901–2100 depicted by world maps of the Köppen-Geiger climate classification. *Meteorologische Zeitschrift*, 19(2), 135–141. <https://doi.org/10.1127/0941-2948/2010/0430>
- Sánchez Cañete, E. P., Kowalski, A. S., Ortiz, P. S., Priego, O. P., & Domingo, F. (2013). Deep CO₂ soil inhalation/exhalation induced by synoptic pressure changes and atmospheric tides in a carbonated semiarid steppe. *Biogeosciences*, 10, 6591–6600. <https://doi.org/10.5194/bg-10-6591-2013>
- Sánchez Cañete, E. P., Ortiz, P. S., Domingo, F., & Kowalski, A. S. (2013). Cave ventilation is influenced by variations in the CO₂ dependent virtual temperature. *International Journal of Speleology*, 42, 1–8. <https://doi.org/10.5038/1827-806x.42.1.1>
- Sanchez-Cañete, E. P., Serrano-Ortiz, P., Kowalski, A. S., Oyonarte, C., & Domingo, F. (2011). Subterranean CO₂ ventilation and its role in the net ecosystem carbon balance of a karstic shrubland. *Geophysical Research Letters*, 38, L09802. <https://doi.org/10.1029/2011GL047077>
- Schimel, D. S. (2010). Drylands in the Earth System. *Science*, 327(5964), 418–419. <https://doi.org/10.1126/science.1184946>
- Serrano Ortiz, P., Roland, M., Moral, S. S., Janssens, I. A., Domingo, F., Goddérís, Y., & Kowalski, A. S. (2010). Hidden, abiotic CO₂ flows and gaseous reservoirs in the terrestrial carbon cycle: Review and perspectives. *Agricultural and Forest Meteorology*, 150, 321–329. <https://doi.org/10.1016/j.agrformet.2010.01.002>
- Takle, E. S., Massman, W. J., Brandle, J. R., Schmidt, R. A., Zhou, X., Litvina, I. V., et al. (2004). Influence of High-Frequency Ambient Pressure Pumping on Carbon Dioxide Efflux from Soil. *Agricultural and Forest Meteorology*, 124(3-4), 193–206. <https://doi.org/10.1016/j.agrformet.2004.01.014>
- Torrence, C., & Compo, G. P. (1998). A practical guide to wavelet analysis. *Bulletin of the American Meteorological Society*, 79(1), 61–78. [https://doi.org/10.1175/1520-0477\(1998\)079<0061:Apgtwa>2.0.Co;2](https://doi.org/10.1175/1520-0477(1998)079<0061:Apgtwa>2.0.Co;2)
- Vargas, R., Baldocchi, D. D., Allen, M. F., Bahn, M., Black, T. A., Collins, S. L., et al. (2010). Looking deeper into the soil: Biophysical controls and seasonal lags of soil CO₂ production and efflux. *Ecological Applications*, 20(6), 1569–1582. <https://doi.org/10.1890/09-0693.1>
- Vargas, R., Collins, S. L., Thomey, M. L., Johnson, J. E., Brown, R. F., Natvig, D. O., & Friggens, M. T. (2012). Precipitation variability and fire influence the temporal dynamics of soil CO₂ efflux in an arid grassland. *Global Change Biology*, 18(4), 1401–1414. <https://doi.org/10.1111/j.1365-2486.2011.02628.x>
- Vargas, R., Sánchez-Cañete, E. P., Serrano-Ortiz, P., Yuste, J. C., Domingo, F., López-Ballesteros, A., & Oyonarte, C. (2018). Hot-Moments of Soil CO₂ Efflux in a Water-Limited Grassland. *Soil Systems*, 2(3), 47. <https://doi.org/10.3390/soilsystems2030047>
- Villarreal, S., Guevara, M., Alcaraz-Segura, D., Brunsell, N. A., Hayes, D., Loescher, H. W., & Vargas, R. (2018). Ecosystem functional diversity and the representativeness of environmental networks across the conterminous United States. *Agricultural and Forest Meteorology*, 262, 423–433. <https://doi.org/10.1016/j.agrformet.2018.07.016>
- Webb, S. W. (2006). Gas transport mechanisms. In C. K. Ho & S. W. Webb (Eds.), *Gas Transport in Porous Media* (pp. 5–26). Netherlands: Springer. <https://doi.org/10.1007/1-4020-3962-X>
- Webb, S. W., & Pruess, K. (2003). The use of Fick's law for modeling trace gas diffusion in porous media. *Transport in Porous Media*, 51(3), 327–341. <https://doi.org/10.1023/A:1022379016613>

- Xu, L., Lin, X., Amen, J., Welding, K., & McDermitt, D. (2014). Impact of changes in barometric pressure on landfill methane emission. *Global Biogeochemical Cycles*, 28, 679–695. <https://doi.org/10.1002/2013GB004571>
- Zamanian, K., Pustovoytov, K., & Kuzyakov, Y. (2016). Pedogenic carbonates: Forms and formation processes. *Earth-Science Reviews*, 157, 1–17. <https://doi.org/10.1016/j.earscirev.2016.03.003>